COMPUTATIONAL FLUID DYNAMICS ANALYSIS OF HELICOPTER DOWNWASH/SHIP AIRWAKE INTERACTION FLOWFIELD

Hüsamettin Alperen ALABAŞ, Yavuz NACAKLI

INTRODUCTION

There are problems specific to the helicopter/ship dynamic interface that limit helicopter operations and cause difficulty associated with landing on a moving platform. Significant factors affecting such operations include visibility, ship motion and aerodynamic interactions of the helicopter with the turbulent airflow near the ship. Associated large velocity gradients and areas of turbulence are limiting operations of helicopter flight onto and from the decks of frigate type air capable ships. For this reason, overcoming the problems that the helicopter encounters as it lands and takes off requires the airflow around the ship and through the helicopter rotors to be well-understood. Ship dynamics, the ship induced airwake, and the aircraft/ship interaction strongly affect the processes such as helicopter takeoff from and landing on shipboards (Bridges et al., 2007). Helicopter shipboard operations impose flight envelope restrictions on the rotorcraft due to a harsher environment. This environment also includes ship airwake caused by ship motion, superstructure, and a respectively smaller landing area. A detailed knowledge of the airflow around the ship and the vicinity of the helicopter rotors are necessary to understand the problems associated with helicopter takeoff and landing. The airwake of the ship includes the region of separated flow on the lee side of the ship's superstructure and hangar door. This region contains steep spatial gradients in flow speed and direction and also contains significant unsteadiness over the bandwidth of concern with respect to handling qualities 0.2-2 Hz (Lee et al., 2013). These characteristics typically have a negative impact on helicopter handling qualities. The time-averaged and unsteady flow phenomena can influence the rotor-generated loads and lead to increased pilot workload (Zan et al., 1994).

NUMERICAL METHOD OF SOLUTION

METHODOLOGY

A four-bladed, 10x6 propeller was used to represent the helicopter rotor to determine the rotor thrust coefficient and the rotor downwash. For the propeller geometry, profiles used from 10 different stations to the root were

taken from the manufacturer. According to these profiles, a 3D propeller model was created in a computer-aided design program. Rotor in isolation was run at freestream velocities range from 0 to 5,14 m/s in hover at rotor rotational speed of 5000 rpm to get the thrust coefficient value. A 2 % simple frigate shape (SFS) model was used to examine the ship's airwake. Although the SFS does not fully reflect the antenna, weapon systems, radar and similar geometries on real ship platforms, it has been demonstrated by experimental studies that the turbulent flow on the deck can be adequately captured (Zan et al., 1994). Isolated frigate simulation was carried out at a freestream velocity of 5.14 m/s at a rotational speed of 5000 rpm in order to give an advanced ratio of 0.075 which replicates a full-scale frigate cruising speed of 60 km/h at 0° deck wind angle.

VALIDATION OF THE METHODOLOGY

ROTOR IN ISOLATION ANALYSIS

In order to determine the validity of the CFD analysis, it is necessary to compare the results with the experimental studies in the literature, and the study of Nacaklı was chosen to determine the accuracy of the CFD simulation to be performed within the scope of this study (Nacaklı, 2010). Propeller and simplified frigate geometry used in the wind tunnel tests and PIV experiments were modeled in computer aided design. Each of PIV velocity field is a time average of 150 images sampled at approximately 3.5 Hz. Vector plots reveals relative velocity magnitudes and direction. Each image represents approximately 24 rotor revolutions at 5000 rpm. All cases are for zero yaw (WOD azimuth = 0 deg), rotor at 5000 rpm, and advance ratio of 0.075 (Nacaklı et al., 2012).

In the sliding mesh method, a rotating volume has to be defined in order to give a rotational motion to the rotor and therefore the disk geometry and hybrid mesh structure in Figure 1 is formed around the rotor.

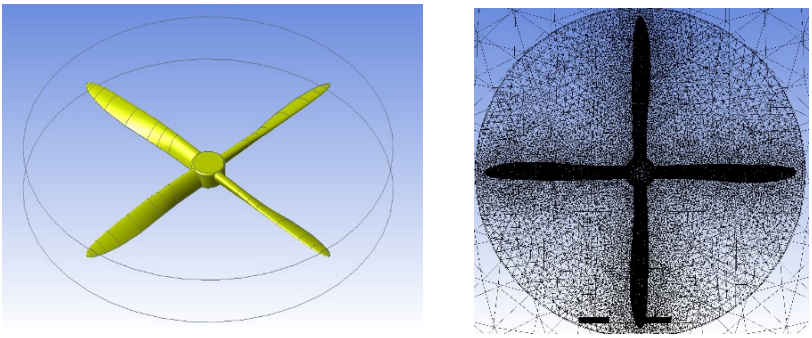

Figure-1. Disk volume and mesh of rotor

Achieving sufficient precision of the speed and pressure variables through the structured mesh on the rotor blade and the vicinity of the rotor is crucial to the success of the simulation. For this reason, the boundary layer was applied around the rotor blade. Thickness of the first layer with these expressions was found to be 5.10^{-5} mm. This thickness together with 1.1 growth rate, 10 boundary layers are created for a blade and hub which close-up view is given in Figure 2.

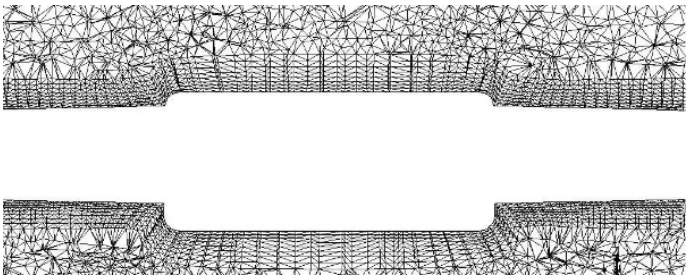

Figure 2. Close-up view boundary layer

Simulations performed with freestream velocities of V_∞ = 0 and V_∞= 5.14 m/s in order to get advance ratios of 0 and 0.075, respectively. The turbulence intensity of the wind tunnel is 0.2% which used for validation of this study. The standard k-ε turbulence model was selected along with improved wall behavior, and the energy equation was included in the solution of the pressure-based and incompressible flow solver. In order to implement the sliding mesh method, the disk volume was given a 5000 rpm rotation in the counter clockwise direction.

Thrust coefficient calculated via the rotor thrust force obtained from simulation results, rotor area and rotor speed. Table 1 shows the differences between the number of elements of the mesh structure and the thrust coefficients obtained with the experimental data.

Table 1. Comparison of mesh element numbers

Mesh Density	Number of Elements (million)	Thrust Coefficient Difference (%)
Coarse	1.9	21.25
Normal	3.6	2.97
Fine	4.8	8.08

The results show that the mesh density of 3.6 million cells is consistent with the wind tunnel result in the literature. It is aimed to find the closest coefficient of thrust for isolated rotor analysis with the determined mesh

structure, zero free flow velocity (J=0) and 5.14 m/s free flow velocity (J=0.075) conditions, for the Spalart-Allmaras and Standard k-ε turbulence models. The comparison of the obtained values with the data in the literature is shown in the Table 2.

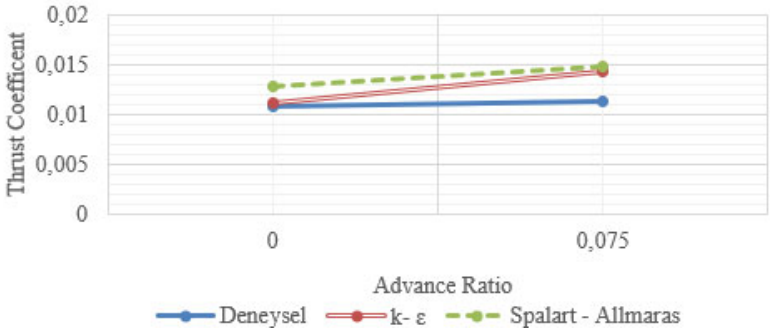

Table 2. Comparison of thrust coefficients according to turbulence models

SHIP GEOMETRY

Simplified frigate geometry, commonly encountered in the literature, was used to represent the ship's platform. The model omits geometric details, instead favouring a simple sharped edged, backward-facing step for minimum Reynolds number dependency. The shape captures the key feature of a frigate in that a landing deck is located downstream of the hangar door. The simplistic geometry allows for fundamental comparisons with CFD simulations (Zan et al., 1994). In this study, 1/50 scale model which is obtained from the experimental study in the literature was created to represent the ship geometry. An unstructured solution mesh was created on the surface of the ship. For a better capture of the flow image on the ship's deck, a more frequent mesh structure has been achieved by increasing the number of points on the lines forming the surfaces on the hangar and deck as shown as in Figure 3.

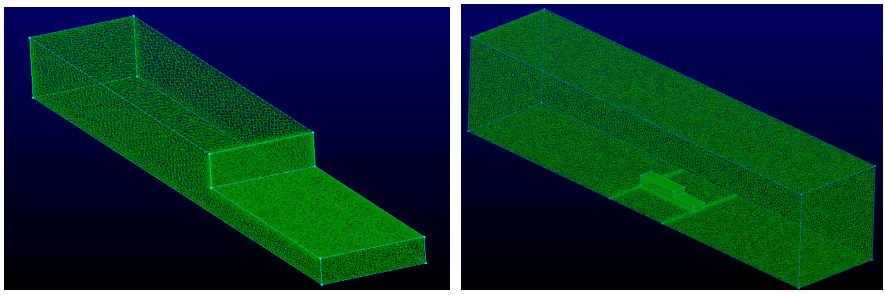

Figure 3. Mesh structure of ship surface and control volume

Width, length and height multipliers used for SFS2 have been preferred in the literature in order to ensure that the opposite wind reaches the ship properly and that the air directed by the ship does not affect the ship again (Orbay, 2016). Thus, the rectangular solution mesh in Figure 3, which is 2.5L in length, 7C in width and 12H in height, is formed in front of and behind the ship, with the length of the ship L, the width C and the height of the hangar H. In the isolated ship solution basin where 867 thousand cells were used, additional nodes were added to the region near the ship and the mesh was densified. All boundary conditions except the velocity inlet and pressure outlet surfaces are defined as walls. Since the ship geometry will be analyzed together with the rotor, Standard k-ε turbulence model has been chosen for the simulation of isolated ship, too. As a result of the simulation, it is seen in Figure 4 that the velocity contour obtained from the deck are close to the experimental study results.

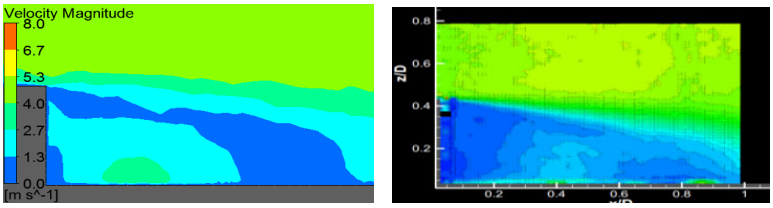

Figure 4. Comparison of CFD (left) and PIV (right) velocity contours

HELICOPTER DOWNWASH/SHIP AIRWAKE INTERACTION

In this section, the dynamic interaction of the flows around the geometries representing the rotor and the ship, whose dimensions and properties have already been stated, is examined. For this reason, the rotor geometry with rotational speed of 5000 rpm under 5.14 m/s freestream velocity was rotated at 9 different locations on the ship's deck to obtain thrust coefficient and flow image. A hybrid solution mesh of 2.7 million elements was created for rotor/ship interaction analysis. The mesh of the disc is positioned on the ship's deck according to the coordinates in which a significant change in thrust coefficient is detected as determined in the study of Nacaklı (Nacaklı, 2010). In the coordinates given in Table 3, the disc diameter (D) is taken as 10.6 inches to prevent the rotating volume from hitting the ship's hangar.

Table 3. Rotor locations

Ratio of Horizontal Distance of the Rotor to Ship Hangar Door to Disc Diameter (x/D)	0.5	0.5	0.5	1.1	1.1	1.1	1.7	1.7	1.7
Ratio of Vertical Distance of the Rotor from Deck to Disc Diameter (z/D)	0.25	0.55	0.75	0.35	0.55	0.75	0.35	0.55	0.75

Mesh of ship and rotor geometry to be used in the simulation of dynamic interaction were created in the same way as in isolated rotor and isolated ship analysis. Therefore, there has been no change of the number of elements in the disk volume and surface of the ship. On the other hand, the area between the disc and the deck of the ship is intensified to provide a more accurate flow image. The dimensions of the solution domain are the same as those of isolated ship analysis. It is aimed to reduce the solution time by reducing the number of elements in remote areas of the solution domain. Mesh to be used in the analysis of dynamic interaction is given in Figure 5.

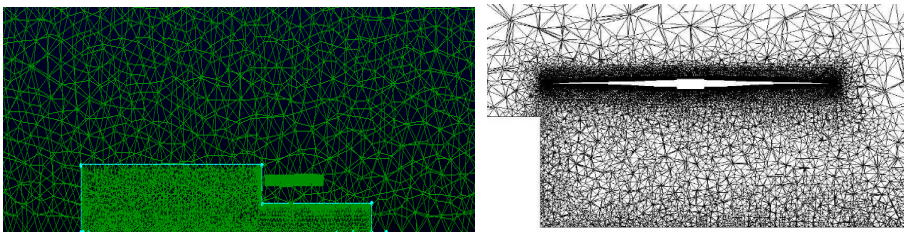

Figure 5. Mesh structure of ship-rotor interaction

Comparison of thrust coefficients obtained from simulations conducted at 3 different rotor heights for x/D=0.5 position with experimental study is given in Table 4.

Table 4. Comparison of thrust coefficients for x/D=0.5

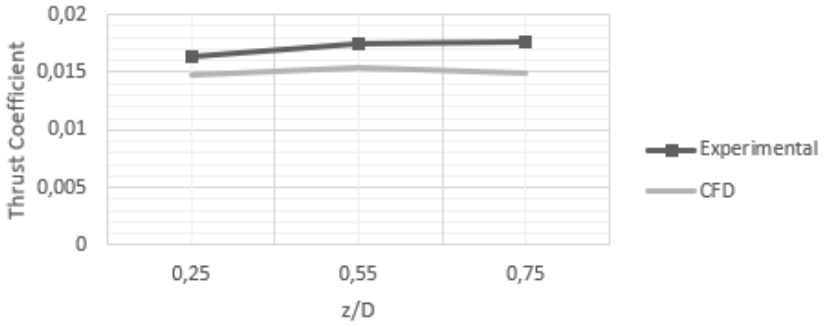

When the rotor is below the top of the hangar door, the recirculation region has a powerful interaction with the rotor wake. The resultant rotor thrust is a product of several influences: the deleterious effect of reingestion, downwash, the relatively low streamwise flow components, and the positive influence of ground effect (Zan, 2002). The flow passing over the top of the

hangar turns downward with the downwash effect of the rotor and recirculation zone and continuous downstream to the stern of the ship. The recirculation zone appears to be smaller and stronger than that of the ship in isolation.

An increasingly larger recirculation zone develops behind the hangar door with increasing rotor height above the deck. Figure 5 presents a sample of the flow field PIV survey results (Nacaklı et al., 2012). In general, the effect of the rotor on the recirculation zone, which exists aft of the hangar, eventually decreases with increasing vertical distance above the landing deck. Recirculation zones are inherently unsteady and thus give rise to the unsteady component of the airwake. As the rotor height increases to a level above that of the hangar door, the thrust coefficient increases due to the increased streamwise flow contribution (Wakefield et al., 2002).

The velocity contour for both PIV and CFD study are given in Figure 5. When compared with the velocity contour in Figure 5 of the experimental study in the literature, it was found that the flow nature was successfully captured. The thrust coefficient is increased with the increase of the freestream flow acting on the rotor rotated at the same distance from the ship hangar horizontally but at a higher position vertically (x/D=0.5; z/D=0.55). According to the flow images, when the rotor rises from the deck, the rotation area also increases.

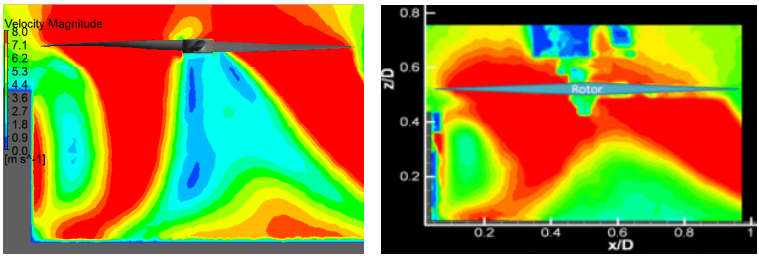

Figure 5. Comparison of CFD (left) and PIV (right) velocity contours (x/D=0.5; z/D=0.55)

In this location where the rotor is behind the ship's hangar, a strong interaction of the rotor downwash with the recirculation zone is observed. It is understood that the thrust is increased due to the ground effect, although the rotor downstream re-enters the rotor.

Comparison of thrust coefficients obtained from simulations conducted at 3 different rotor heights for x/D=1.1 position with experimental study is given in Table 5, and when the comparison is taken into consideration, it is understood that the trend of thrust coefficient can be captured.

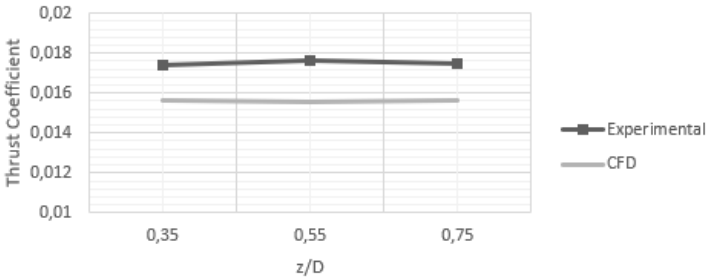

Table 5. Comparison of thrust coefficients for x/D=1.1

The velocity contour for rotor position of x/D = 1.1; z/D = 0.35 for both PIV and CFD study are given in Figure 6, respectively. The results obtained are consistent with the velocity contours obtained from the experimental study. When the rotor moves from the hangar door to the stern of the ship, it is seen that the stagnation line moves along the horizontal axis.

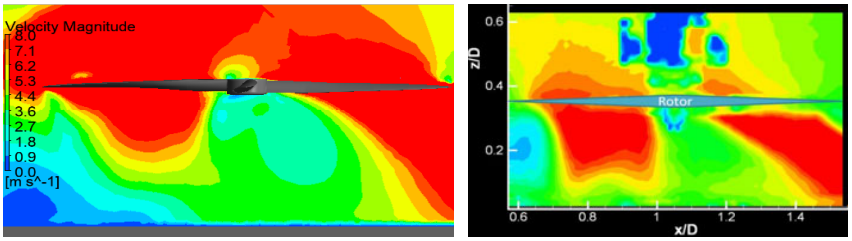

Figure 6. Comparison of CFD (left) and PIV (right) velocity contours (x/D = 1.1; z/D = 0.35)

When the thrust coefficient comparison is examined for x/D=1.7 position which is given in Table 6, it is seen that the thrust tendency trend can be captured in the simulations at three different heights made for the farthest position of the rotor on the horizontal axis.

Table 6. Comparison of thrust coefficients for x/D=1.7

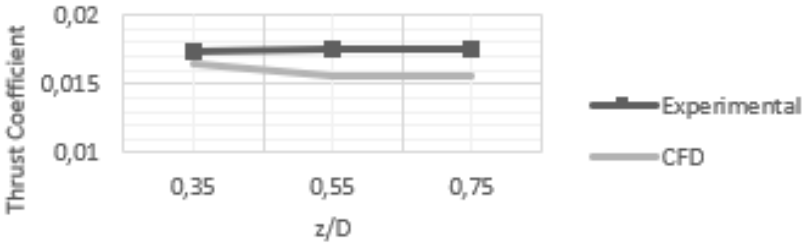

The velocity vectors and velocity contour for rotor position of x/D = 1.7; z/D = 0.75 for both PIV and CFD study are given in Figure 7. The results obtained are consistent with the velocity contours obtained from the experimental study. In this position of the rotor, it is seen that the recirculation region is formed on the deck and the effect of the downwash of the rotor decreases as it moves away from the deck.

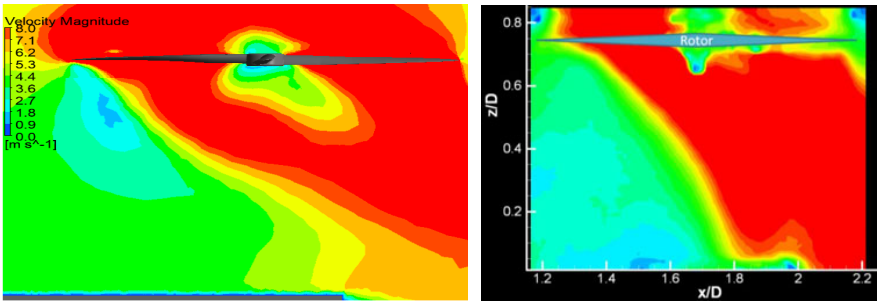

Figure7. Comparison of CFD (left) and PIV (right) velocity contours (x/D = 1.7; z/D = 0.75)

RESULTS

Helicopter operations on the ship become very challenging for pilots by adding flow directed by the helicopter rotor to the turbulent flow created by the ship's superstructure on the deck. Therefore, it is very important to understand the interaction of the flow around the helicopter rotor with the ship's airwake. In this study, isolated rotor geometry at two different advance ratios was investigated with k-ε and Spalart-Allmaras turbulence models in hybrid mesh structure. The results obtained from time-dependent simulations were compared with PIV and thrust coefficient data in the literature. Although the Spalart-Allmaras turbulence model gives a more consistent velocity distribution for the lower region of the isolated rotor with PIV images, it is considered that it does not capture pressure gradients well for the thrust coefficient. Isolated ship simulation was performed with k-ε turbulence model under freestream velocity of 5.14 m/s given at 0° wind on deck angle to represent cruise speed. The flow contour was compared with the PIV images in the literature. It has been seen that the basic features of turbulent air caused by ship's superstructure can be successfully reflected. In the simulations performed for unsteady k-ε turbulence model, the flow separation in the rotor downwash results in less ground effect and therefore lower thrust coefficient for rotor conditions under ship airwake than in the experimental study. This also increases the recirculation zones on the deck. In addition, where the rotor is in close proximity to the ship's deck, the

thrust coefficient difference with the experimental study decreases and the similarity between the flow images increases. In this study using sliding mesh method, the distances between the ship deck and the rotor were slightly higher than the experimental study due to the size of the disk volume created for rotor rotation. This situation is considered to increase the differences in thrust coefficient and flow images. On the other hand, when the thrust coefficients obtained for 9 different rotor locations are examined, it is seen that dynamic interaction and ground effect can be determined and the propensity of the thrust coefficient in the experimental study can be captured.

REFERENCES

Bridges, D.O., Horn, J.F., Alpman, E. and Long, L.N. (2007), "Coupled Flight Dynamics and CFD Analysis of Pilot Workload in Ship Airwakes", AIAA Atmospheric Flight Mechanics Conference and Exhibit, Hilton Head South Carolina.

Lee, R.G., and Zan, S.J. (2013), "Wind Tunnel Testing of Unsteady Loads on a Helicopter Fusulage in a Ship Wake", 23rd Congress of the International Congress of the Aeronautical Sciences, Toronto, Carnada.

Zan, S.J., and Gary, E.A. (1994), "Wind Tunnel Measurements of the Airwake Behind a Model of the Generic Frigate", NRC-IAR-LTR-AA.

Nacaklı, Y. (2010), "Analysis of Helicopter Downwash/Frigate Airwake Interaction Using Statistically Designed Experiments", Ph.D. Th., Old Dominion University, USA.

Nacaklı, Y., Landman, D. and Doane, S. (2012), "Investigation of Backward-Facing-Step Flowfield for Dynamic Interface Application", Journal of the American Helicopter Society, 57(3), pp.1–9.

Orbay, E. (2016), Computational Fluid Dynamics Simulations of Ship Airwake with a Hovering Helicopter Rotor (yüksek lisans tezi), ODTÜ,

Wakefield, N.H., Newman, S.J., and Wilson, P.A. (2002), "Helicopter Flight Around a Ship's Superstructure", Proceedings of the Institution of Mechanical Engineers, Part G: Journal Aerospace Engineering, 216, pp.13

Zan, S.J. (2002), "Experimental Determination of Rotor Thrust in a Ship Airwake", Journal of the American Helicopter Society, 47(2), pp.100–108.